Journal Pre-proof

Exploring the relationship between urban form and land surface temperature (LST) in a semi-arid region Case study of Ben Guerir city - Morocco

Rida AZMI , Cédric Stéphane TEKOUABOU KOUMETIO ,
El Bachir DIOP , Jérôme Chenal

PII: S2667-0100(21)00208-0
DOI: https://doi.org/10.1016/j.envc.2021.100229
Reference: ENVC 100229

To appear in: *Environmental Challenges*

Received date: 21 April 2021
Revised date: 27 July 2021
Accepted date: 28 July 2021

Please cite this article as: Rida AZMI , Cédric Stéphane TEKOUABOU KOUMETIO , El Bachir DIOP , Jérôme Chenal , Exploring the relationship between urban form and land surface temperature (LST) in a semi-arid region Case study of Ben Guerir city - Morocco, *Environmental Challenges* (2021), doi: https://doi.org/10.1016/j.envc.2021.100229

Highlights

- The study area had the inverse effect of surface urban heat island
- Residential areas like open low rise contribute to the decrease of surface temperature
- Green infrastructure solutions are the most suitable in semi-arid areas
- Temperature difference between urban and peri-urban areas is increasingly worrying
- Statistical approaches (ANOVA, spatial clustering) precisely quantify the differences

Exploring the relationship between urban form and land surface temperature (LST) in a semi-arid region Case study of Ben Guerir city - Morocco

Rida AZMI [a]
Mohammed VI Polytechnic University – UM6P
Center of Urban Systems - CUS
Ben Guerir, Morocco
Rida.azmi@um6p.ma

Jérôme Chenal [b]
Ecole Polytechnique Fédérale de Lausanne - EPFL
Suisse
jerome.chenal@epfl.ch

Cédric Stéphane TEKOUABOU KOUMETIO [a]
Mohammed VI Polytechnic University – UM6P
Center of Urban Systems - CUS
Ben Guerir, Morocco
stephane.koumetio@um6p.ma

El Bachir DIOP [a]
Mohammed VI Polytechnic University – UM6P
Center of Urban Systems - CUS
Ben Guerir, Morocco
elbachir.diop@um6p.ma

Abstract: Surface temperature is one of the critical factors used to study microclimate conditions through Land surface Temperature (LST), a widely used data source. This paper tests a classification approach using moderate spatial satellite resolution images to extract surface properties of Local Climate Zones (LCZs) in a semi-arid region against measured LSTs. However, LST is used to study and explore the spatial relationship between temperature and urban morphology. Therefore, it is considered an alternative and reliable data source to complement in-situ measurement, especially in developing countries.

The used methodology is based on two statistical approaches: 1) auto-spatial correlation using Getis Ord Gi* statistic, and 2) ANOVA test. Results showed an inversion effect of surface urban heat island - SUHI, where a strong correlation between specific LCZs and the surface temperature was found. The urban classes represented by open-low-rise, compact-low-rise have shown a significant decrease in surface temperature for almost two decades and in both summer and winter seasons compared to non-urban ones.

Therefore, the outcomes of this study may have critical implications for urban planners who seek to mitigate SUHI effects in arid and semi-arid urban areas. Also, the approach used in this study can be helpful to follow the urban environment's spatial and temporal development as an application framework of sustainable development.

Keywords: Land surface temperature, Remote Sensing, Analysis of Variance, Spatial-autocorrelation, Sustainable Development

1 Introduction

Urbanized areas are among the most affected by climate variability, and the degree to which the issues present on the territory include buildings, infrastructure, population, activities, etc. However, the impacts of climate change have already begun to affect the climate significantly and make places of habitat vulnerable [1]. The concept of vulnerability to climate change is defined in the Intergovernmental Panel on Climate Change Assessment Report – (IPCC) as " the degree to which a system is likely to be adversely affected by the effects of climate change without being able to cope with them " [2]. Therefore, climate change can be considered as a common problem, requiring joint collaborative action between all the stakeholders. As a result, several countries have started to readjust their agendas with new agreements; this is shown in the United Nations Framework Convention on Climate

Change (UNFCCC) of 2015, followed by the COP22 from a previous COP21 fundamental advance were recorded.

In practical terms, cities generally cause and experience these warming phenomena and are thus the front line in the fight against climate change. Consequently, climate change will affect both urban and rural populations, and it is in the cities that the effects will be felt the hardest. As a result, they will experience the most significant temperature increases, particularly to urban heat islands – (UHIs), whose products are amplified by human activities. Although the phenomenon of UHI has been known for more than 200 years, it has gained media attention in the last decade. Initially, the greenhouse effect directly enhances the heat island effect as a driver of smaller-scale climate change.

The UHI effect influences the climate of the city, although the town generates it, its morphology, its materials, its natural, climatic, and meteorological conditions, its activities...etc. However, the UHI effect is an urban fact to be considered in the design and management of the city.

When thermal remote sensing is used to analyze the UHI effect, Surface Urban Heat Island (SUHI) is used instead. In this work, we are interested in surface temperature, where the SUHI effect is an essential indicator of the urbanization consequences and has rapidly changed cities' dynamics. Therefore, accurate measurements of the impacts and changes resulting from the SUHI may provide helpful information for urban planning [3-5]. These heat islands form because urban surfaces such as roadways and rooftops absorb and emit heat to a greater extent than most natural surfaces [6].

Land Surface Temperature - (LST) is considered an excellent alternative to carry out the information gap and to complete the missing data in areas where weather stations are less existing [7]. It is generally used to estimate surface temperature from indirect measurements of surface radiation, upward thermal radiance, and surface emissivity using thermal remote sensing [8, 9]. In addition, LST is considered an essential parameter of microclimatic conditions and can be accessed free of charge and globally through satellite images. Thus, LST is one of the most important environmental parameters used for determining the exchange of energy and matter between the surface of the earth and the lower layer of the atmosphere.

There are several ways to retrieve LST using satellite images [10-15], where LST data is affected by four mains factors:1) land surface type, 2) surface moisture, 3) illumination, and

4) atmospheric conditions. The advantage of using satellite images for retrieving LST is high spatial resolution and temporal frequency for a large area [16]. However, many studies showed the reliability of LST data based on satellite images instead of in-situ measurements [17-19].

Understanding the urban thermal environment is vital for improving urban planning and strategy development when mitigating urban heat islands. However, LST acquired from satellite images can be used to study the temperature characteristics of Local Climate Zones – (LCZ) classes by providing continuous data on surface temperature[20] . The effect of urban development on local thermal climate is widely documented in scientific literature. The classification of urban environments into LCZs allowed a deeper understanding of urban dynamics [21] . In addition to its substantial usefulness in urban climate studies, LCZ provides additional data for applications such as disaster mitigation, urban planning, and population assessment [22] . With its ability to provide accurate data on the urban environment, LCZ also provides reference information for achieving Sustainable Development Goal [23]. LCZ classification can be considered as a good combination of accuracy, low-time consuming, and low-cost mapping method, especially for cities without land use/land cover (LULC) maps, despite some zones' misclassification.

Arid and semi-arid areas such as the Marrakech-Safi region in Morocco are highly vulnerable to increased drought frequency and intensity, they will be most severely affected by water scarcity in the future [24]. Thus, this study aims to analyze the variations in LST due to urban land cover types in Ben Guerir city using Landsat images from 2004 to 2020; to identify and understand the peculiarities of the urbanized semi-arid environment concerning LST.

For this reason, we started this work to provide a quantitative framework on soil temperature variations resulting from different LCZ over Benguerir city and the surrounding areas.

The specific research objectives include:

- Constructing a database based on LST time series to visualize the actual magnitude of LST changes between 2004 and 2020 ;
- Applying Ord Getis G* statistic on LST change data to extract urban temperature clusters (hot spots vs. cold spots) and to detect the spatial pattern of such statistically significant temperature;
- Interpreting the transformation of urban morphology using LCZ classes integrating statistical approaches.

Finding the balance between the urban thermal environment and human activities is critical in the heat island effect mitigation strategy. Thus, several researchers have tried to find a significant relationship between urban sprawl and the urban heat island effect. And this, through physical measurements from different sources of data [25].

Several works presented LST as an indicator to study the urban dynamics against the surface heat island phenomenon. These works can be categorized into two main contributions:

Authors have proposed a Framework based on a purely statistical approach to study the differences between LCZs using LST [26]. Generally, researchers used moderate to high spatial resolution data combined with large scale vector data [27-30]. Other works have inserted vegetation indices (VI) as an additional parameter, and a main component of an urban ecosystem [31, 32]. Using very high spatial resolution data is also proposed [33, 34] . However, they started from the premise that the higher the resolution, the more accurate the data are and the more accurately they can reveal variation on a local scale. All previous works used simple linear models to test the impact of LST in each LCZ. However, a second category is an approach combining statistical analysis and spatial autocorrelation techniques [35-37]. The findings are convincing, with a certain limitation: the remote sensing images' spatial resolution. Thus, the following researchers used different spatial resolution images [38]. While other authors used moderate to high spatial satellite images in the most vulnerable areas suffering from semi-arid and arid climates [39, 40].

2 Material and Methodology

2.1 Study area

Ben-Guerir city (32.23680, -7.950349) is part of Rhamna, a predominantly rural subdivision of the region Marrakech – Safi - MS. As mentioned in figure 1B, Ben- Guerir located in the north of the region MS, where the province area is characterized by rugged terrain, and it is 445 m above sea level. The study area is characterized by a semi-arid climate with minimum temperatures ranging between 4.3° and 5.1° C and maximum ranging from 37.5 to 39.3 °C. Rainfall remains among the lowest recorded in Morocco, which means an increasingly structural drought [41]. The province contains the Rhamna massif and the Gantour plateau, which constitutes a significant phosphate wealth. However, Ben-Guerir city considered a futuristic city targeted by the Office Chérifien du Phosphate – OCP group (which is a Moroccan company specialized in mining exploration) to become an innovative and sustainable city [42]. Studying the spatial and temporal variations of the local climate can contribute to the proper orientation of the development projects of the old city, as well as the green city. However, understanding the evolution of the LCZ through surface temperature allows all stakeholders to have key information on one of the climate parameters that can be used to support their future decisions.

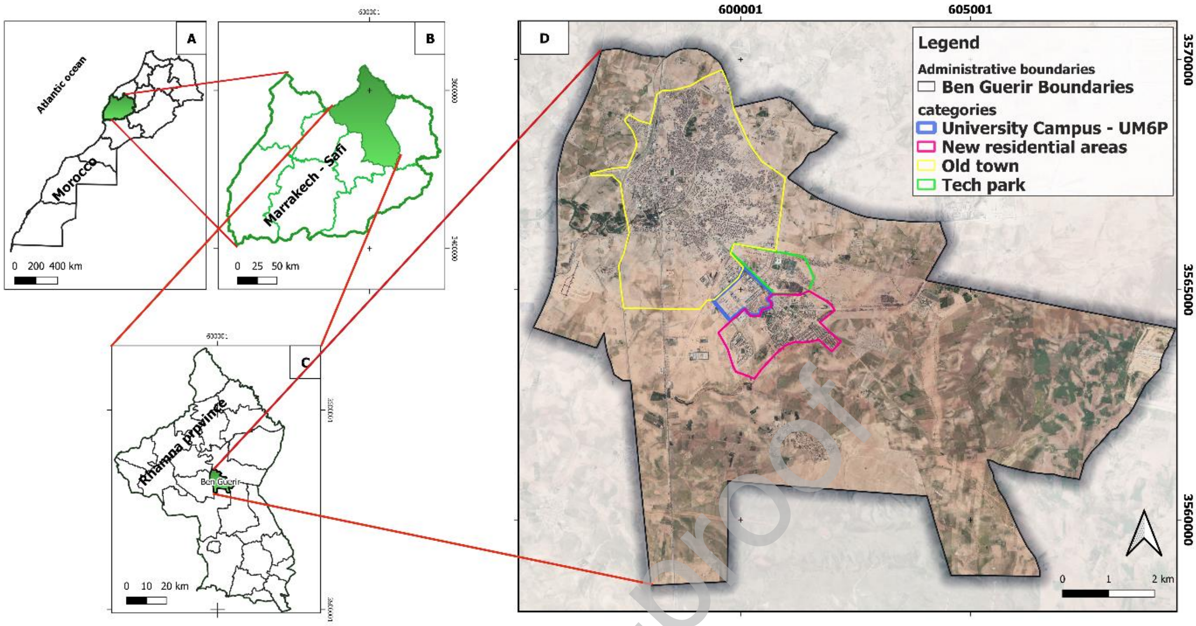

Figure 1. Ben Guerir city (D) and the surrounding areas in relation to its province (A) and region (B).

2.2 Methodology

The Methodology used in this paper is composed mainly of three processing steps, as mentioned in the workflow (figure 2). A pre-processing first step of Landsat satellite images is used to estimate LST data and to execute the classification of LCZ maps. The second one consists of validating the classification results for the LCZ and processing the LST by affecting the temperature value of each class. Finally, applying the statistical approach to study and analyze the behavior of surface temperature in each urban structure. In this case, two statistical approaches were adopted: The first consists of using local spatial association method indicators based on Ord Getis G* statistic [43], this method used to discover the spatial pattern by drawing a particular focus on identifying temperature hot spots and cold spots as spatial outliers. Thus, the second approach completes the analysis of the previous spatial pattern and evaluates the differences in surface temperature using LCZ classes.

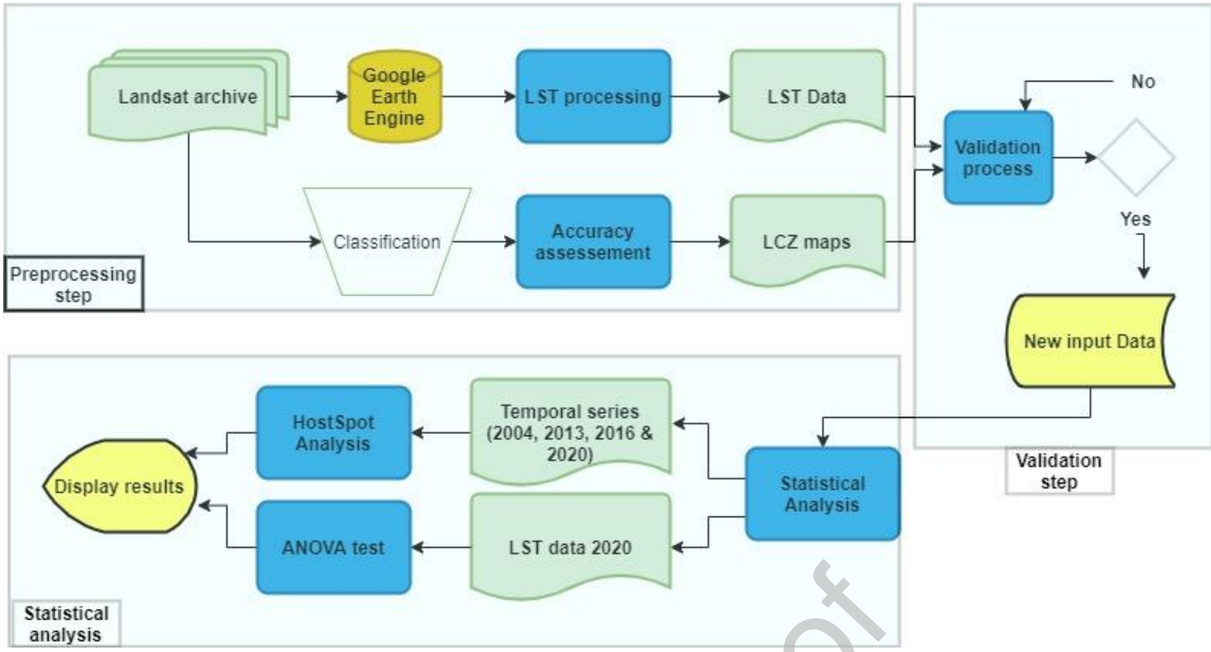

Figure 2. Flowchart of the study

2.2.1 Hot Spot Analysis calculation

The concept behind hot spot analysis is to identify statistically significant spatial clusters composed of high values (hot spots) and low values (cold spots). The analysis generally groups feature when high or low similar values are found in a cluster. The hot spot analysis concept works by looking at each feature in the dataset within the context of neighboring features in the same dataset. This processing allows the creation of new output data with a z-score, a p-value, and a confidence level bin for each entity.

In the literature, there are several methods to study and understand the distribution of a phenomenon, particularly to know more specifically whether (or not) there are clusters of high/low values. The most used are local techniques, where they prevailed because of their ability to identify locations with elevated values. In this case, we reviewed two famous techniques, 1) Getis-Ord Gi* [43] , and Local Moran's I [44] . The choice of the appropriate method generally depends on the main question in our research, which is finding high values surrounded by high values.

Local Moran's I technique only indicates that similar values occur together, and it does not indicate whether any cluster is composed of high or low values. By contrast, Getis-Ord GI* statistic can indicate whether high or low values are concentrated over the study area. However, by finding general G statistic, we can significantly measure statistic points surrounded by a concentrated point that are statistically significant.

2.2.2 Analysis of variance

Analyzing whether there is a significant difference between the LCZ class and the LST values is used to reconcile the variations better. In other words, the study focuses on whether values of LST are more likely to take place in some LCZ classes rather than others. A simple linear model is applied to assess the mathematical relationship between LCZ class ~ LST-values in the summer and winter seasons. ANOVA test is applied to check if differences are statistically significant by comparing LST values among LCZ classes.

2.3 Data preprocessing

2.3.1 Land surface temperature estimation

Several studies have shown the usefulness and quality of LST data from the Landsat constellation [45, 46]. The spatial and temporal resolution of the Landsat series is largely sufficient to study the phenomenon at a regional and global scale [47] . The method presented by Sofia Ermida [48] is adopted in this study consisting of the estimation of LST data using the Google Earth Engine - (GEE) platform. The authors provided a code repository that allows computing LSTs from Landsat 4, 5, 7, and 8 within GEE. The proposed workflow used the Statistical Mono-Window - (SMW) algorithm developed by [49] where the algorithm uses the brightness temperature - (BT) of the thermal infrared - (TIRS) band, mean and difference in land surface emissivity for estimating the LST of an area as mentioned in equation (1) :

$$\mathbf{LST} = \frac{\mathbf{BT}}{\mathbf{1}} + \mathbf{W} * \left(\frac{\mathbf{BT}}{\mathbf{p}}\right) * \mathbf{ln}(\mathbf{e}) \quad \textbf{(1)}$$

Where,
LST = Land surface temperature in Kelving
BT = brightness temperature at satellite temperature in Kelving
W = Wavelength of emitted radiance
p = h*c/s (1.438*10-2 mk)
h = Plank's constant ($6.626*10^{-34}$ Js)
s = Boltzmann constant ($1.38*10^{-23}$ J/K)
c = Velocity of light (2.998*108 m/s)
p =14380

Mono-windows algorithm has two main advantages: 1) easy to implement and calibrate, and 2) it uses a single thermal band. GEE platform allows two other datasets, which are essential to calculate the emissivity value at the pixel level. The first one is atmospheric data from the re-analyses of the National Center for Environmental Prediction - (NCEP) and

National Center for Atmospheric Research - (NCAR) [50]. The NCEP re-analysis is the only global Total Column Water Vapor - (TCWV) dataset available on GEE that covers the full period of operations of the Landsat series. The second database is surface emissivity from the Advanced Spaceborne Thermal Emission and Reflection Radiometer Global Emissivity Database - (ASTER GED) developed by the National Aeronautics and Space Administration's - (NASA) and Jet Propulsion Laboratory - (JPL) [51] .

2.3.2 Local Climate Zones classification

Based on the photointerpretation of very high spatial satellite resolution images and the city's development plan, the categorization process allows the classification of different LCZs. Protocol for LCZ extraction at level 0 is described by Wang & Ren [52], allowing a satellite-based method. A pixel-based supervised classification approach with a random forest algorithm has been used to extract LCZ classes [53]. The first operation in manipulating raw data consists of digitizing the training areas for the supervised classification using Landsat data [54] . The classification was calculated and conducted by the random forest classifier based on similarities between the training samples and the rest of the study area [55] . The procedure used is universal and characterized by several criteria that aim to obtain a simple treatment method to use, fast, and without associated cost.

For more accuracy, the Google Earth images were regarded as the reference data, which is accurate enough to reflect the proper land cover to validate the classification result. Training areas are obtained according to the characteristics of the LCZ classification system given by [20]. Seven classes of 17 possible classes were found, and Table 1 shows the classes found in the study area with a brief description of LCZs. Thus, figure 3 shows different urban structures in the study area. Most of the city's morphology comprises the low-compact-rise and small vegetated areas. Other urban forms in the south are composed of neighborhoods of open-low-rise areas, were tiny houses with high standing architecture. Besides, the region's semi-arid nature allows the lightweight rise as a dominant class around the city. There are some irrigated plantations in the south of the city for green areas, which are considered low-planting classes and forestry plantations to combat desertification in the region. To facilitate displaying the following graphs and the interpretation of the results, LCZ classes have been re-coded. Table 1 presents the new coding adopted, which will be used in the following sections.

Table 1. Local Climate Zone (LCZ) classes retained and recorded for Ben Guerir city based on (Stewart and Oke, 2012) classification.

ID	Class	Description
01	Compact Low – Rise	Small buildings with a very dense structure, and the vegetation cover is almost zero
02	Open Low – Rise	Buildings of medium standing made up of average areas of habitat. The vegetation cover is present with a spaced road network
03	Lightweight Low – Rise	It is a group of dwellings very well known in the Maghreb countries, bringing together individuals linked by a kinship based on a common ancestry in paternal line.
04	Scattered trees	Scattered trees generally are forest plantations all around the city
05	Low plants	Multi-annual crops grown by farmers in peri-urban areas
06	Paved or Rock areas	Areas with a rocky structure that appears in black in satellite images / or paved areas, like the one in the military base near the city
07	Bare soil or Sand	Considered any land use that remains in the image

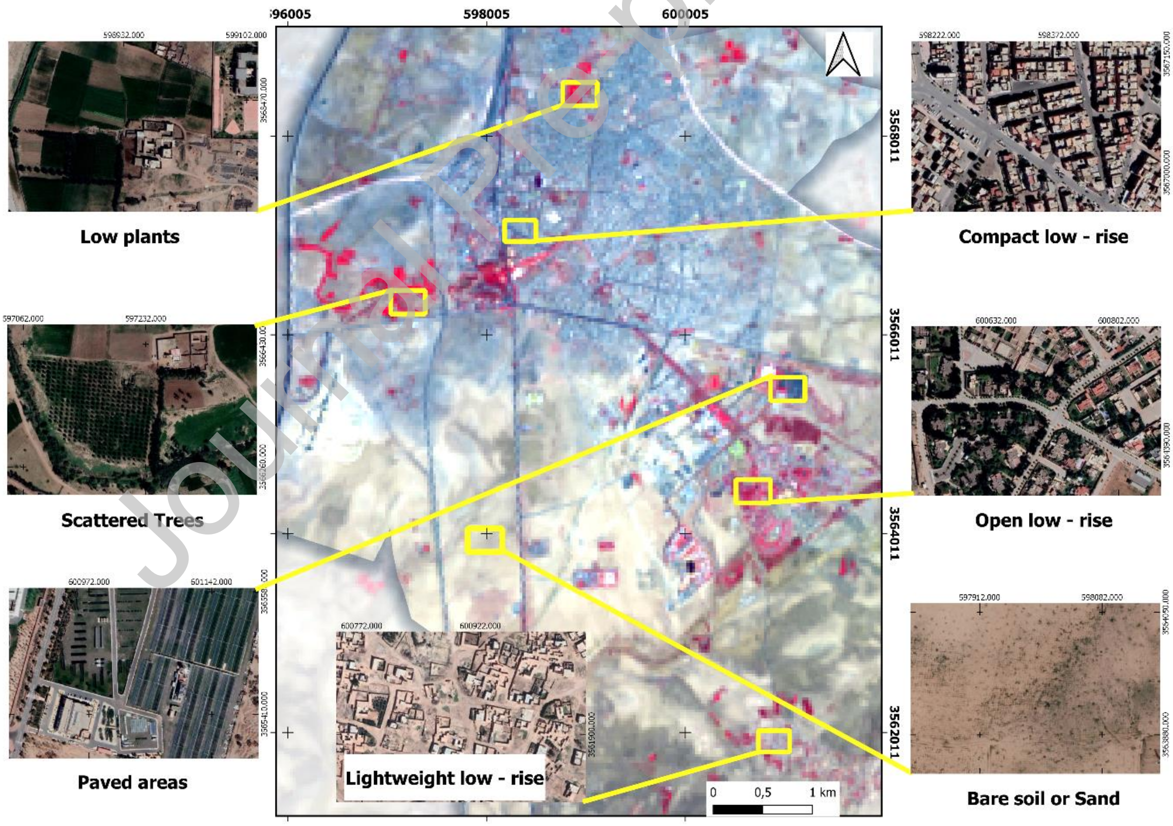

Figure 3. Local Climat Zone (LCZ) classes found in Ben Guerir city and the surrounding areas over false color Landsat image

3 Results and discussion

The classification of LCZs was carried out on 4 successive dates (2004, 2013, 2016 and 2020). As mentioned above, the training plots are ground truth polygons based on a digitization on Google earth Images. The result are thematic maps with the 7 proposed classes with a spatial resolution of 100m. Table 2 shows the accuracy assessment for each date, where overall accuracy was higher than 0.7 in 2004, 2013, and 2016, except for 2020, which gave an overall accuracy of 62%. Also, the degree of confusion between the classification result and the ground truth is shown in table 2, where the diagonal matrix indicates good accuracy in different classes. A refinement allowed to increase even more the precision of final classification by doing a manual adjustment of the marginalized classes classified pixels. In this improvement process, Google Earth images used as a reference and up to date data. Figure 4 shows different classification of LCZ maps after the refinement.

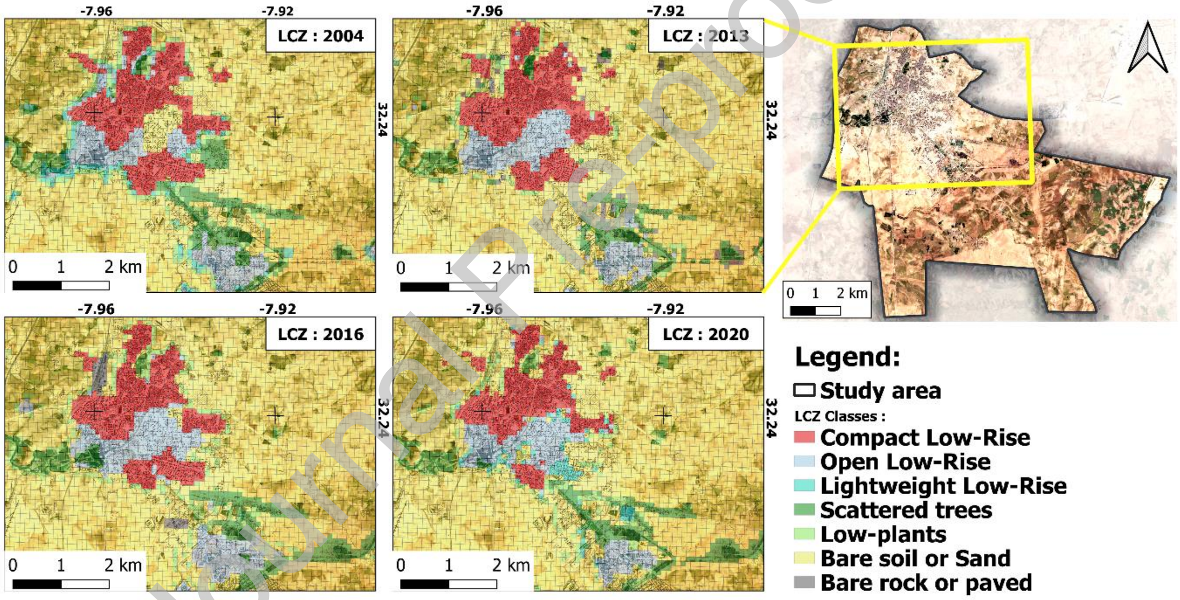

Figure 4. Thematic maps of LCZ classes after manual enhancement (2004, 2013, 2016 and 2020)

Table 2. Contingency matrix for each LCZ class (between 2004 and 2020) – ***UA*** : User Accuracy, ***PA*** : Producer Accuracy, ***OA***: Overal Accuracy

Yrs	***Classes***	***UA***	***PA***	***OA***		***PA***	***UA***	***OA***		***PA***	***UA***	***OA***		***PA***	***UA***	***OA***
2004	Compact Low - Rise	93.3 %	100 %	75 %	**2013**	82.4 %	70 %	75 %	**2016**	55.6 %	93.8 %	71 %	**2020**	69.4 %	86.2 %	62 %
	Open Low – Rise	78.6%	19 %			0.0	-			5.6 %	91.7			-	-	
	Lightweight Low – Rise	33.9 %	58.3 %			13.2	28.4 %			37.8 %	8.2			10.4	60 %	
	Scattered trees	20 %	20 %			-	-			13.3 %	12.5 %			100	6.2 %	
	Low plants	97.8 %	88.1 %			100%	61.7 %			77.8 %	16.7 %			-	-	
	Paved or Rock areas	-	-			-	-			-	-			100	88.39 %	

	Bare soil or Sand	96.4 %	83.5 %			95 %	76.7 %			89.3 %	88.9 %			99.4	81.2 %	

As shown in figure 5, the surface of bare soil is dominant in the study area, of which it covers 70%, followed by a low vegetation cover of 10% composed mainly of plants scattered in the form of green spaces in the city and wild plants in the surroundings. The urban classes represented by the open-low-rise, which we see a slight increase in area between 2004 and 2020, followed by the lightweight, low rise class with a decrease due to the national policy to combat slums and unstructured housing [56]. Thus, the compact-low-rise class has seen stagnation with a slight increase between 2016 and 2020. The class of scattered trees has experienced an increase due mainly to the projects of planting green spaces to increase the rate of vegetation cover and the rate of renewal of forests, fight against erosion, and maintain the ecological balance of the territory.

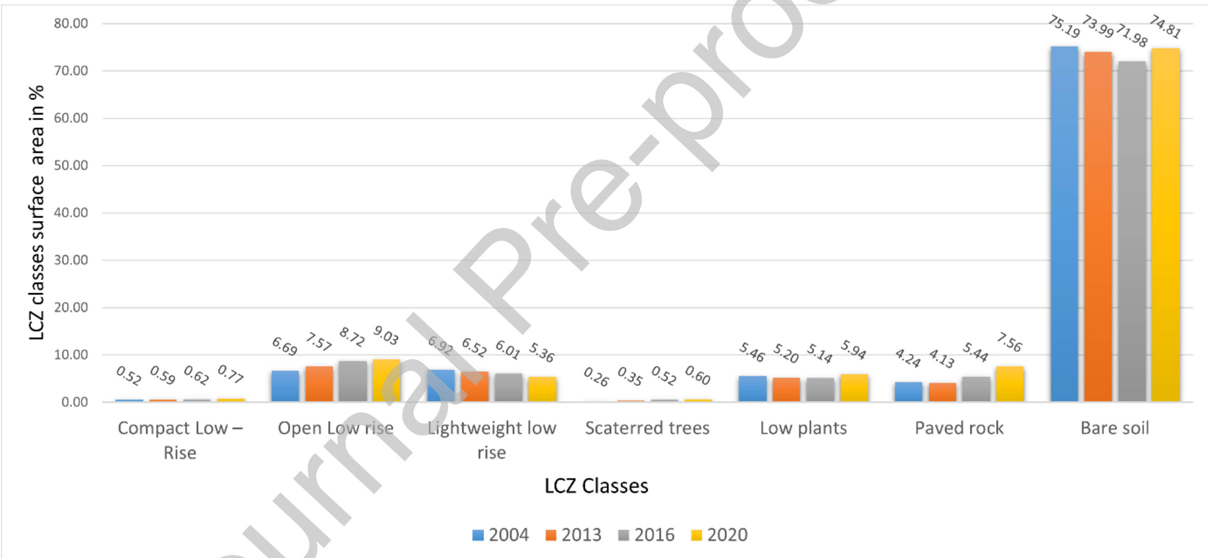

Figure 5. Histogram presenting the corresponding surface area (in %) of each LCZ in the four scenarios

3.1 Descriptive statistics

To statistically analyze the variation and identify the relationship between LST values and LCZ classes, a set of 350 samples were taken from the different land cover types. We used a sampling based on spatially distributed points to avoid using the whole image. The study area is composed of an urbanized area of small size compared to the peri-urban areas, and the use of pixel integrality (with peri-urban dominance) may bias the statistical population, resulting in a poor quantification of spatial temperature variation.

Figure 6 shows the surface temperature variation in different LCZ classes, and different pattern based on the average temperature. The year 2013 was marked by a high temperature across all classes. The report given by the World Meteorological Organization - (WMO) [57] can explain the high values in that particular year. However, the same year was one of the five hottest years between 2011 – 2015 ever recorded globally. The temperature was 0.57°C (1.03°F) above the normal for the reference period (1961-1990) [57].

The average temperature showed in figure 6 varies according to the nature of the urban structure. However, these variations generally have a downward pattern, where average temperature values have decreased by one to two degrees between 2004 and 2020. The most notable classes that experienced a significant drop in temperature are bare soil, compact-low-rise, and open-low-rise. However, the bare soil class is less warm in winter when the average temperature is rising (between 2004 and 2020). On the other hand, it is descending in summer. This rise in temperature in winter is probably due to the nature of the soil in the region. From a geological perspective, the province is characterized by the Rhamna massif, composed of ornamental rocks such as green marble, and building materials such as quartz and silica sand.

Another variation of temperature was noticed in the urbanized areas (more particularly, open-low-rise and compact-low-rise classes). A descending average temperature is noticed; this is generally explained by potential relationship between impervious surfaces and LST values. Changes in surface temperatures are very dependent on urban dynamics, more specifically on changes in urban form. In this case, the city has experienced rapid urbanization and a spread of impervious surfaces starting from 2010. Consequently, new neighborhoods and structures like compact-low-rise appear parallel with type open-low-rise habitats in the city's southeast. The redevelopment works done by OCP group around the new green city, especially the university campus, and the projects surrounding them has contributed to the decrease of surface temperature. The statistics do not show a great variation between the different years; and the distribution of the average temperature values does not show the variations since most of the averages between the different classes are close together.

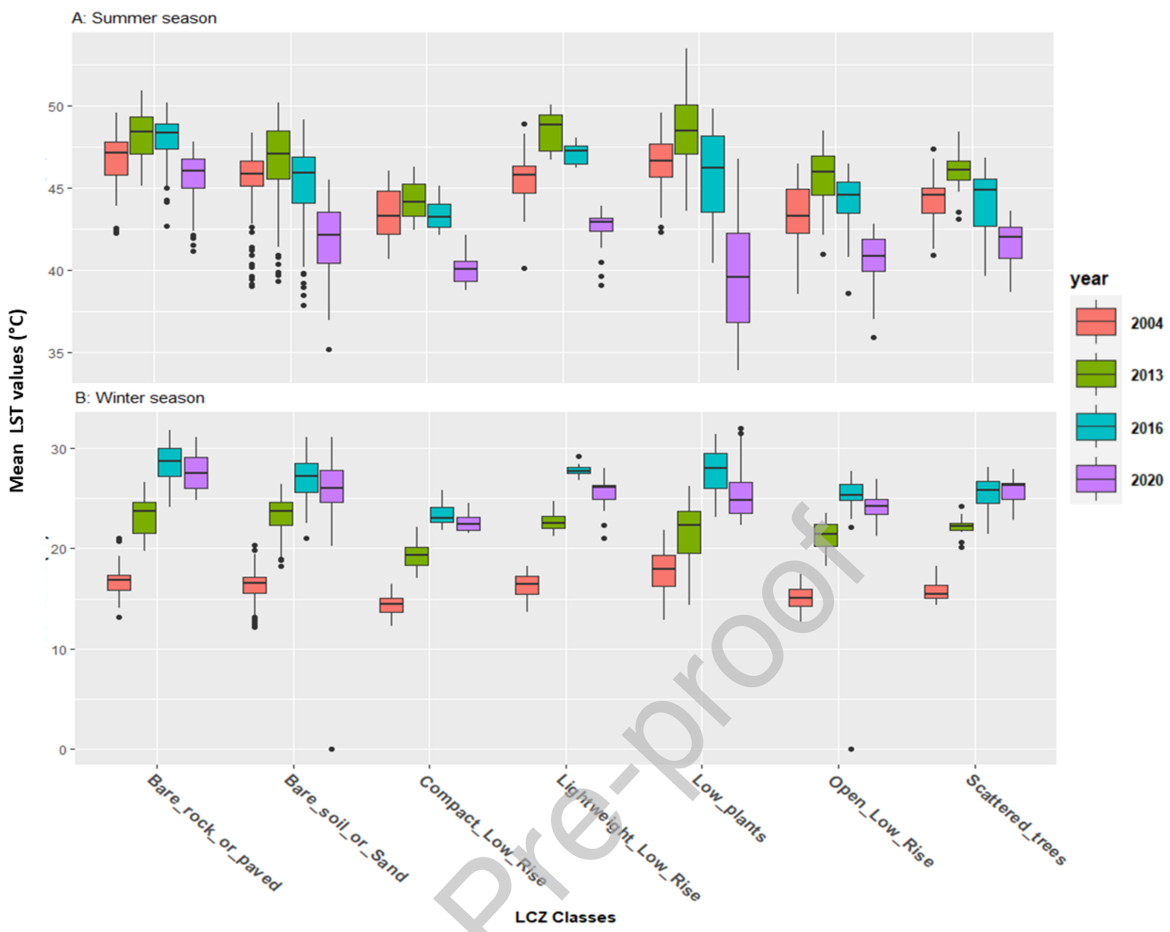

Figure 6. LST value by LCZ classes (2004, 2013, 2016 & 2020), A) for summer, & B) for winter.

3.2 The impact of bare areas on LST in arid and semi-arid regions

Surface urban heat island - (SUHI) presented by the difference between LST in urban relativity to bordering non-urban surfaces is used [58, 59]. Furthermore, the SUHI intensity indicator was computed using equation (2):

$$SUHI = LST_{urban} - LST_{sub\text{-}urban} \qquad (2)$$

LST_{urban} represents the mean LST for the different urban form, and $LST_{sub\text{-}urban}$ represents the mean LST of the surrounding areas. In this study, the bare-soil class considered a sub-urban area and all other classes considered as urban.

Temperature differences showed that bare soil has higher LST values compared to urbanized areas. Table 3 shows differences in both seasons where the most significant differences are seen in the summer, particularly in compact-low-rise and open low-rise classes successively in 2004 and 2013, followed by 2016 and 2020. On the other hand, large negative values are captured in the winter of years (2013, 2016, and 2020) compared to a low negative value in 2004. These SUHI inversions show the seriousness of the heat island phenomenon and its development over time in a semi-arid area. For the lightweight-low-rise class, the difference is generally positive in all years, and the probable explanation is that there is a spectral confusion between these urban structures and the bare soil. However, lightweight-low-rise is generally made up of buildings with local materials of the exact nature as the bare ground's existing components. The lightweight-low-rise class that is generally isolated in the bare ground allows the surface temperature of the bare ground to impact it and negatively influence it.

Table 3. Difference for SUHI in summer and winter season

Classes / years	Differences in summer				Differences in winter			
	2004	2013	2016	2020	2004	2013	2016	2020
Bare rock or paved	1.395	1.558	2.708	3.676	0.379	0.121	1.473	1.77
Compact Low-Rise	-2.031	-2.32	-1.781	-1.791	-2.003	-3.825	-3.602	-3.266
Lightweight Low-Rise	0.166	1.909	1.942	0.713	0.084	-0.616	0.773	-0.22
Low-plants	1.282	1.9	0.614	-1.937	1.493	-1.79	0.811	-0.288
Open Low-Rise	-1.955	-0.948	-1.045	-1.323	-1.206	-2.041	-2.195	-1.525
Scattered trees	-1.095	-0.668	-1.027	-0.256	-0.5	-1.013	-1.389	0.012

These temperature differences validate that the SUHI has a reverse effect and a general influence on the urban environment. These findings are consistent with the works of Parvez & Abulibdeh [60, 61]. They showed that the Spatio-temporal variations of the LST in semi-arid climate have an inverse effect due to the nature of the peri-urban areas, which have soil with desert characteristics.

Another explanation that allows bare soil to have higher LST values than urbanized surfaces is heat concentration, sparse vegetation cover, low relative humidity, and topsoil aridity in the upper layers of the sandy soil. During the summer, the sandy soil has lower water content and a faster depletion rate, which leads to a higher LST. Bare soil in this area is characterized by sandy soil, characterized by lower water holding capabilities and smaller thermal inertia. On the contrary, other types of soils, such as clay soil used for planting have higher water-holding capabilities. Thus, the higher the water content in the soil, the slower the depletion rate, which results in a lower LST.

Previous results on the average distribution of LST values in Figure 6 shows an overlap between the surface temperature and the classes being different in terms of LST values. At this stage, we cannot judge whether the observed differences are random or there is a fundamental difference that is statistically significant.

However, we employed two statistical approaches to answer the question related to the relationship between urban morphology and LST. The first one is a spatial method, which consists of performing a hot-spot analysis by calculating each dataset entity's Getis Ord G* statistic [62]. The second approach is purely attributive, and it is based on a linear model. Thus, the approach evaluates the relationship in its entirety between groups that correspond to the modalities of a qualitative variable (LCZ classes) and the calculated averages from a continuous variable (LST values).

3.3 Hotspot & cold spot analysis

The process is repeated in the four scenarios, both in summer and winter. All significant hot spots are identified by a high z-score and a low p-value. Unlike, all cold spots are identified by a low negative z-score and a small p-value. Figure 7 shows the spatiotemporal pattern of hot and cold spots using the LST variable between 2004 and 2020. After calculating the Getis Ord G* statistics, results are presented where hot and cold spots were classified into seven categories based on their Gi_Bin values: very hot spot, hot spot, and warm spot, which have successive significance levels (99%, 95%, and 90%). Not statistically significant is an isolated class, and finally, a cool spot, cold spot, and very cold spot have successive significance levels (99%, 95%, and 90%).

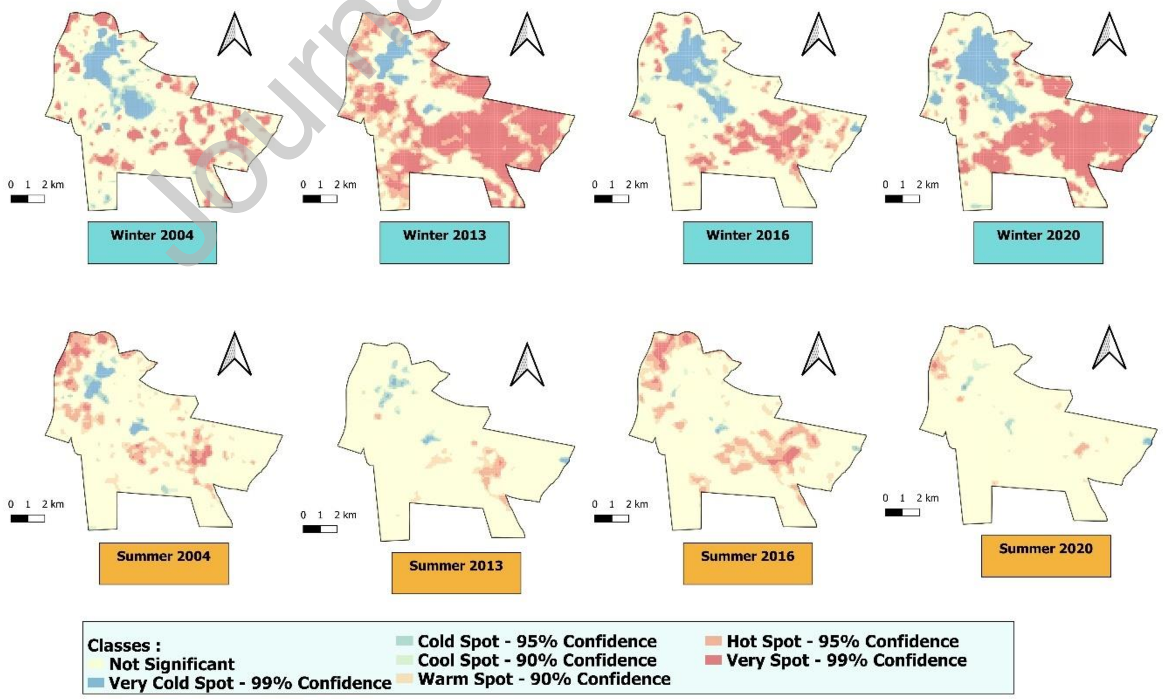

Figure 7. Hot Spot Analysis using Getis Ord G* method

Descriptive statistics relating to hot and cold spots and their spatial representation are shown in figure 8 and histograms in appendix A. The whole area is covered by a variation of thermal anomalies. Considering the total areas of the clusters in terms of surface area - (SA), the figure in appendix *A* shows the percentages of the total hot and cold spot areas in each year. In winter, the cold spot area is almost half of the hot spot area except for the year 2013 where the cold spot area is too small. On the other hand, in summer, we notice that the cold spot areas have increased between 2004 and 2020.

The histogram in figure 8 represents the spatial and temporal variation of the sum of the mean temperatures in all the cold and hot spots areas. Figure 8A shows the variations in summer with little variation in cold spots compared to the hot zones. On the other hand, the winter period (figure 8B) had a typical trend with decreasing values between (2004 and 2020), particularly in cold spots. In exchange, cold spots have been grouped generally in urbanized areas where the compact-low-rise class is presented. The same thing for the summer season, a cluster of cold spots over urbanized areas, more particularly in the south of the city whose open-low-rise class is present.

The overlay of the LCZs map on the clusters and the monitoring of changes in land use have shown that most bare soil areas had become reforested areas or areas built on the new green city of Ben Guerir. This analysis of land use validates the downward trend in temperature between 2004 and 2020. However, the changes encountered in the clusters and represented by constructing the University Mohammed IV Polytechnic (UM6P) campus and its entire integrated ecosystem with the surrounding projects, located in the heart of the new green city between 2013 and 2020. The obtained results enable us to assume that the redevelopment and reforestation around the city between 2010 and 2020 have contributed to the decrease in surface temperature.

The pattern analysis using clustering with a single parameter (the surface temperature) is insufficient to explain the relationship between LST and changes in cities' urban morphology. However, a second statistical approach is used to deepen the analysis and find the spatial relationship.

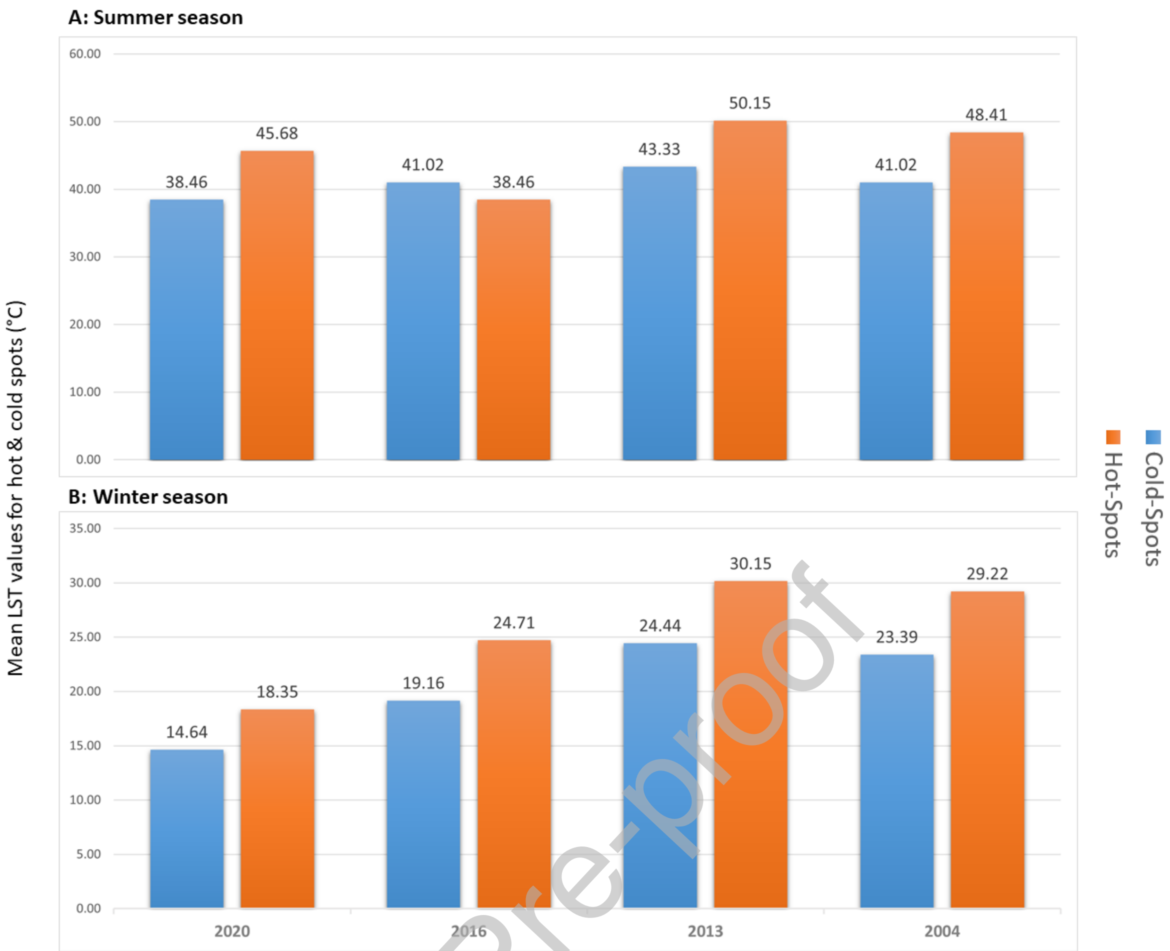

Figure 8. Mean LST values for total Hot & Cold spots in each year (A) for summer and (B) for winter

3.4 ANOVA test

Analyzing whether there is a significant difference between the LCZ class and the LST values is used to reconcile the variations better. In other words, the study focuses on whether values of LST are more likely to take place in some LCZ classes rather than others. A simple linear model is applied to assess the mathematical relationship between LCZ class ~ LST-values in the summer and winter seasons. ANOVA test is applied to check if differences are statistically significant by comparing LST values among the seven LCZ classes.

Basically, the normality of data has been verified, and the plot in figure 9 draws the correlation between the defined dataset and the normal distribution. However, it shows the Shapiro-Wilk test calculation for each class, where the p-value is more significant than 0.05, and all points lie approximately along the reference line for each cell.

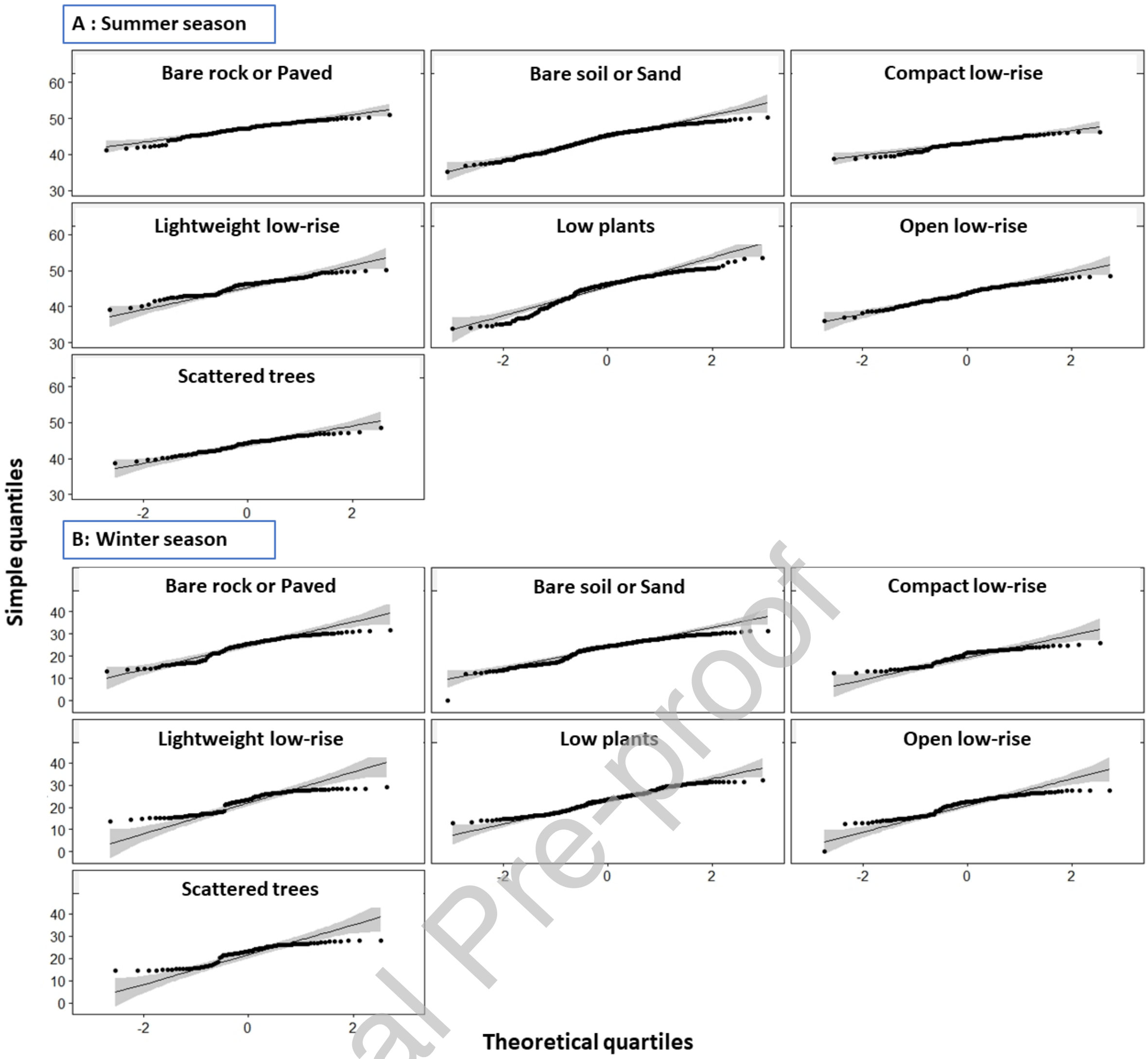

Figure 9. QQPlot showing the normality of the dataset, A) for summer & B) for winter

The variation of LST means among different LCZ classes is much larger than the variation of LST within each class, and the p-value is less than 0.05. However, a significant difference was validated by the ANOVA test. A post hoc pair comparison is applied to determine which groups are different from the others. Figure 10 shows LCZ class pairs' visualization and analysis of significant differences by plotting the ANOVA metrics where significant differences do not cross the zero value. The method uses a conservative error estimate to find the statistically different groups from one another [63].

Post hoc test revealed the unique combinations that have a significant difference. However, LST values were statistically significantly different between the different classes, except for the differences between bare-soil and paved areas (7-6), another non-significant difference between scattered trees and lightweight-low-rise (4-3), and bare soil and lightweight-low-rise (7-3). The findings obtained from the ANOVA test show a potential relationship between some LCZ classes and the LST. The model generally shows that urban areas (compact and open-low-rise) substantially impact LST values.

Class	ID
Compact Low-rise	01
Open low-rise	02
Lightweight low-rise	03
Scattered trees	04
Low plants	05
Paved or Rock	06
Bare soil or Sand	07

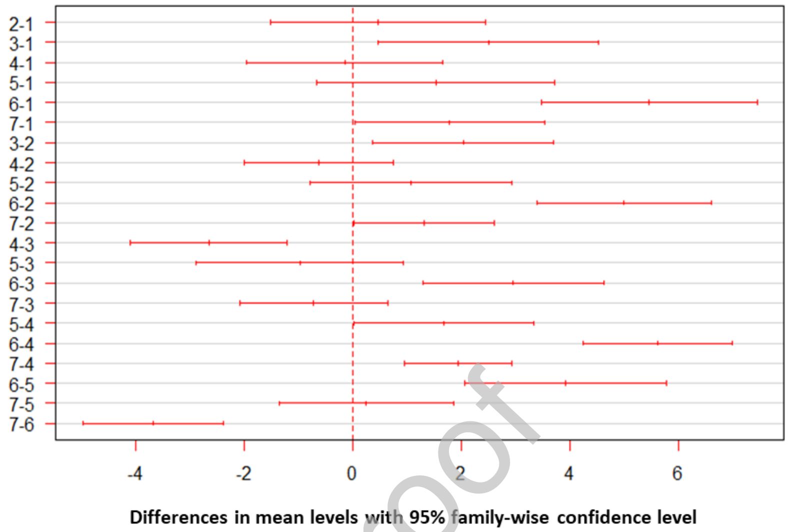

Figure 10. Pair comparison of LST value means using LCZ classes

3.5 Discussion

The comparison test comes to validate the results obtained previously in section 3.2, saying that the urban classes that constitute the core of Ben Guerir city's morphology positively impact and contribute to the decrease of the temperature.

Spatial autocorrelation showed the behavior of surface temperature towards the urban and peri-urban fabric. The appearance of hot spots in permeable surface areas and cold spots in impermeable areas indicates the inverse effect of SUHI in semi-arid regions. The statistical approach based on the ANOVA test showed the different classes with a statistically significant relationship with surface temperature.

A comparison between our findings and similar work done on Tehran, Iran, in 2016 [58] showed almost the same conclusions on the terrestrial thermal behavior in a semi-arid climate. The authors approved that peri-urban areas have a higher surface temperature than urbanized areas; They used medium resolution data to evaluate SUHI in a semi-arid climate (over several seasons in the year). Then, they employed three SUHI indicators, i.e., LST difference, Land use /Land cover and fractional vegetation cover. As a result, authors showed that the higher temperature in barren lands/soils around the city contributed to the generation of a surface urban cool island, particularly in the daytime.

In our study, we used large-scale data compared to previous studies. Thus, the spatial autocorrelation allowed to better specify the statistically significant areas with their ground truth. The spatio-temporal analysis showed that the urbanized areas have a descending pattern of concentration of hot spots in summer. Our findings show the reverse effect of SUHI in this semi-arid zone and agree with the findings of Parvez [40] which he used the same data source of Landsat constellation between (1991 and 2016). The main objective was to identify and understand the peculiarities of the urbanized desert environment in relation to LST in the desert city of Jeddah in Arabie Saudia. The author has shown that his findings agree with other studies mentioning that the increase of LST is duo to human activities. On the other hand, the effect of increasing vegetation cover might have been overridden by more intensive human activities and extensive urban expansion in 2015/2016 which has decreased temperature.

A second search by [64] in a metropolitan city of Ahmedabad in India shows that the rural zone exhibits a higher average LST than the urban area, especially in the summer season. To assess the impact on SUHI variations, an ancillary data composed of land cover maps, normalized differential vegetation index, surface albedo, evapotranspiration, urban population, and groundwater level across the years are used. Results showed that the negative SUHI intensity is due to the low vegetation present in the rural area, dominated by croplands turning into bare land surfaces during the pre-monsoon summer season. In our case, the vegetation cover of the area is too low, especially in summer, which causes intensive surface heat gain. These temperatures are in general more elevated with respect to the urbanized zones of which the vegetal cover is moderate.

3.5.1 Limitation

Application of the statistical approaches to examine the relationships between multi-temporal LSTs and urban morphology has research merit, but also certain limitations: (i) In this study, the need to improve Land Surface Emissivity (LSE) estimation in urban areas, where LSE is one of the main factors affecting the accuracy of the LST estimation [65]. However, emissivity varies with the impervious surface, which was not considered in the current sub-pixel estimation method. (ii) To give more accurate LST values over urban areas, the use of an in situ validation where LST obtained from satellite measurements is directly compared to LST from ground measurements, and the absolute difference between both variables can be investigated and analysed.

4 Conclusion

A case study of spatial variation of urban morphology was performed to analyze the LST spatiotemporal characteristics using RS images. Statistical models were used to examine the relationships between the LSTs and LCZs. The main conclusions are as follows:

- The results mentioned above will encourage future construction works espacially in new green city to adopt a sustainability strategy based on materials that allow the absorption (even if partial) of urban heat;
- The semi-arid climate has its own characteristics which are presented in rising temperatures and more extreme, unpredictable climate events which making sustainable livelihoods tough for many people living in those regions. However, investment in urban green infrastructure - (GI) approach by supporting building resilience, mitigating greenhouse gases emissions can help to reduce artificial heat;
- Supporting the use of climate information in the local context in order to apply co-production of knowledge, and to improve scientific research in arid and semi-arid zones by including a range of stakeholders to think about the problem together.

As a recommandation, future studies allowing for the urban–rural diference method with analysis of LST variations and their relationships with biophysical factors like (NDVI, and Evapotranspiration - ET) to help urban planners to formulate site-specific mitigation strategies. It may also be possible for future studies to use large-scale data from mobile or fixed sensors for mesuring LST data in the future green city of Ben Guerir.

The use of satellite data to build a knowledge base with archived data of more than 40 years that will help to understand the spatial and temporal variations of the phenomenon; the cross-referencing of these data with economic factors and other climatic and biophysical parameters in order to make in-depth analyses of past changes and make the right decisions for future interactions of decision makers.

Funding

This research did not receive any specific grant from funding agencies in the public, commercial, or not-for-profit sectors.

Declaration of Competing Interest

The authors declare no conflict of interest.

Appendix A

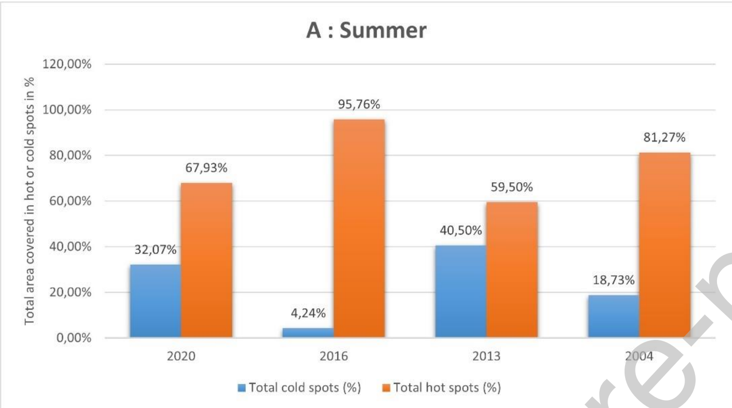
A : Summer
Total area covered in hot or cold spots in %
120,00%
100,00%
80,00%
60,00%
40,00%
20,00%
0,00%
32,07%
67,93%
4,24%
95,76%
40,50%
59,50%
18,73%
81,27%
2020
2016
2013
2004
Total cold spots (%)
Total hot spots (%)


A : Winter
Total area covered in hot or cold spots in %
100,00%
90,00%
80,00%
70,00%
60,00%
50,00%
40,00%
30,00%
20,00%
10,00%
0,00%
35,29%
64,71%
35,29%
64,71%
7,41%
92,59%
36,32%
63,68%
2020
2016
2013
2004
Total cold spots (%)
Total hot spots (%)

References

[1] R. Heltberg and M. J. W. B. p. r. w. p. Bonch-Osmolovskiy, "Mapping vulnerability to climate change," *World Bank policy research working paper,* vol. no. WPS 5554 Washington, D.C. : World Bank Group., no. 5554, 2011.

[2] D. Q. Thomas F. Stocker, Gian-Kasper Plattner , Melinda M.B. Tignor , Simon K. Allen, Judith Boschung, Alexander Nauels, Yu Xia , Vincent Bex, Pauline M. Midgley, "GIEC, Résumé à l'intention des décideurs, Changements climatiques 2013: Les éléments scientifiques. Contribution du Groupe de travail I au cinquième Rapport d'évaluation du Groupe d'experts intergouvernemental sur l'évolution du climat," in "Cambridge University Press, Cambridge, Royaume-Uni et New York (État de New York), États-Unis d'Amérique," 2013.

[3] L. F. Kucukali, "Applications of satellite image index values to obtain the relation of land use and urban heat island effect," (in English), *Fresenius Environmental Bulletin,* Article vol. 29, no. 10, pp. 8869-8883, 2021.

[4] X. Liang, X. Ji, N. Guo, and L. Meng, "Assessment of urban heat islands for land use based on urban planning: a case study in the main urban area of Xuzhou City, China," (in English), *Environmental Earth Sciences,* Article vol. 80, no. 8, 2021, Art. no. 308.http://dx.doi.org/10.1007/s12665-021-09588-5

[5] J. Yang, Y. Wang, C. Xiu, X. Xiao, J. Xia, and C. Jin, "Optimizing local climate zones to mitigate urban heat island effect in human settlements," (in English), *Journal of Cleaner Production,* Article vol. 275, 2020, Art. no. 123767.http://dx.doi.org/10.1016/j.jclepro.2020.123767

[6] S. Peng *et al.*, "Surface urban heat island across 419 global big cities," *Environ Sci Technol,* vol. 46, no. 2, pp. 696-703, Jan 17 2012.http://dx.doi.org/10.1021/es2030438

[7] Y.-j. Jeong, S.-i. Lee, J.-h. Lee, S. D. Jin, S. H. Son, and W. Choi, "Development of numerical land surface temperature model of Jeju Island, South Korea based on finite element method," (in English), *Environmental Earth Sciences,* Article vol. 80, no. 9, 2021, Art. no. 357.http://dx.doi.org/10.1007/s12665-021-09645-z

[8] G. Rongali, A. K. Keshari, A. K. Gosain, and R. J. P. J. S. T. Khosa, "A mono-window algorithm for land surface temperature estimation from Landsat 8 thermal infrared sensor data: a case study of the Beas River Basin, India," vol. 26, no. 2, pp. 829-840, 2018.

[9] Y. Yuhendra and J. T. S. Sumantyo, "Assessment of Landsat 8 TIRS data capability for the preliminary study of geothermal energy resources in West Sumatra," (in English), *TELKOMNIKA (Telecommunication Computing Electronics and Control),* Article vol. 18, no. 5, pp. 2737-2747, 2020.http://dx.doi.org/10.12928/telkomnika.v18i5.16172

[10] L. F. Peres, C. C. J. I. T. o. G. DaCamara, and R. Sensing, "Emissivity maps to retrieve land-surface temperature from MSG/SEVIRI," vol. 43, no. 8, pp. 1834-1844, 2005.

[11] J. A. Sobrino, J. C. Jiménez-Muñoz, and L. J. R. S. o. e. Paolini, "Land surface temperature retrieval from LANDSAT TM 5," vol. 90, no. 4, pp. 434-440, 2004.

[12] F. Arabi Aliabad, M. Zare, and H. Ghafarian Malamiri, "Comparison of the accuracy of daytime land surface temperature retrieval methods using Landsat 8 images in arid regions," *Infrared Physics & Technology,* vol. 115, p. 103692, 2021/06/01/ 2021.http://dx.doi.org/10.1016/j.infrared.2021.103692

[13] J. Cristóbal, J. Jiménez-Muñoz, A. Prakash, C. Mattar, D. Skoković, and J. Sobrino, "An Improved Single-Channel Method to Retrieve Land Surface Temperature from the Landsat-8 Thermal Band," *Remote Sensing,* vol. 10, no. 3, 2018.http://dx.doi.org/10.3390/rs10030431

[14] J. C. Jiménez-Muñoz and J. A. Sobrino, "A generalized single-channel method for retrieving land surface temperature from remote sensing data," (in English), *Journal of Geophysical Research: Atmospheres,* Article vol. 108, no. D22, pp. ACL 2-1 - ACL 2-9, 2003.http://dx.doi.org/10.1029/2003jd003480

[15] T. Song *et al.*, "Comparison of four algorithms to retrieve land surface temperature using Landsat 8 satellite," (in Chinese), *Yaogan Xuebao/Journal of Remote Sensing,* Article vol. 19, no. 3, pp. 451-464, 2015.http://dx.doi.org/10.11834/jrs.20154180

[16] C. Qiu, L. Mou, M. Schmitt, and X. X. Zhu, "Local climate zone-based urban land cover classification from multi-seasonal Sentinel-2 images with a recurrent residual network," *ISPRS J Photogramm Remote Sens,* vol. 154, pp. 151-162, Aug 2019.http://dx.doi.org/10.1016/j.isprsjprs.2019.05.004

[17] M. F. Abdulateef and H. A. Al-Alwan, "Assessment of surface urban heat island intensity and its causes in the city of Baghdad," in *IOP Conference Series: Materials Science and Engineering*, 2020, vol. 745, no. 1, p. 012162: IOP Publishing.

[18] R. H. AL-Anbari, O. Z. Jasim, and Z. T. Mohammed, "Estimation High Resolution Air Temperature Based on landsat8 images and Climate Datasets," in *IOP Conference Series: Materials Science and Engineering*, 2019, vol. 518, no. 2, p. 022033: IOP Publishing.

[19] M. El-Hattab, A. S.M, and L. G.E, "Monitoring and assessment of urban heat islands over the Southern region of Cairo Governorate, Egypt," (in English), *The Egyptian Journal of Remote Sensing and Space Science,* Article vol. 21, no. 3, pp. 311-323, 2018.http://dx.doi.org/10.1016/j.ejrs.2017.08.008

[20] I. D. Stewart and T. R. Oke, "Local climate zones for urban temperature studies," (in English), *Bulletin of the American Meteorological Society,* Article vol. 93, no. 12, pp. 1879-1900, 2012.http://dx.doi.org/10.1175/BAMS-D-11-00019.1

[21] S. J. Quan and P. Bansal, "A systematic review of GIS-based local climate zone mapping studies," (in English), *Building and Environment,* Review vol. 196, 2021, Art. no. 107791.http://dx.doi.org/10.1016/j.buildenv.2021.107791

[22] B. Bechtel *et al.*, "Towards consistent mapping of urban structures - Global human settlement layer and local climate zones," 2016, vol. 41, pp. 1371-1378: International Society for Photogrammetry and Remote Sensing.

[23] U. J. N. Y. U. N. Nations, Department of Economic and S. Affairs, "Transforming our world: The 2030 agenda for sustainable development," 2015.

[24] T. F. Stocker, D. Qin, G.-K. Plattner, M. Tignor, S.K. Allen, J. Boschung, A. Nauels, Y. Xia, V. Bex and P.M. Midgley (eds.), "IClimate Change 2013: The Physical Science Basis. Contribution of Working Group I to the Fifth Assessment Report of the Intergovernmental Panel on Climate Change, IPCC," in "Cambridge University Press, Cambridge, United Kingdom and New York, NY, USA, ," 2013, vol. 1535 pp.

[25] B. Bechtel *et al.*, "Mapping Local Climate Zones for a Worldwide Database of the Form and Function of Cities," (in English), *ISPRS International Journal of Geo-Information,* Article vol. 4, no. 1, pp. 199-219, 2015.http://dx.doi.org/10.3390/ijgi4010199

[26] A. Prata Shimomura and A. Ferreira, "LCZ in Metropolitan Regions: Surface Temperature in urban and rural areas," in *PLEA 2018 Conference*, 2018, pp. 796-801.

[27] Z. Cai, G. Han, and M. Chen, "Do water bodies play an important role in the relationship between urban form and land surface temperature?," (in English), *Sustainable Cities and Society,* Article vol. 39, pp. 487-498, 2018.http://dx.doi.org/10.1016/j.scs.2018.02.033

[28] M. Kaikai, L. Yan, Z. Moyan, H. Bing, and Y. Liu, "Investigations of Surface Urban Heat Island Effect Based on Local Climate Zone Method: A Case of Xi'an," 2019, vol. 136: EDP Sciences.

[29] J. Quan, "Multi-Temporal Effects of Urban Forms and Functions on Urban Heat Islands Based on Local Climate Zone Classification," (in English), *Int J Environ Res Public Health,* Article vol. 16, no. 12, Jun 17 2019, Art. no. 2140.http://dx.doi.org/10.3390/ijerph16122140

[30] F. Zullo, G. Fazio, B. Romano, A. Marucci, and L. Fiorini, "Effects of urban growth spatial pattern (UGSP) on the land surface temperature (LST): A study in the Po Valley (Italy)," (in English), *Sci Total Environ,* Article vol. 650, no. Pt 2, pp. 1740-1751, Feb 10 2019.http://dx.doi.org/10.1016/j.scitotenv.2018.09.331

[31] A. Rida, S. Abderrahim, and K. Ilias, "Estimation of spatial distribution and temporal variability of land surface temperature over Casablanca and the surroundings of the city using different Landat satellite sensor type (TM, ETM+ and OLI)," *International Journal of Innovation and Applied Studies,* vol. 11, no. 1, pp. 49-57, 2015.

[32] L. S. Ferreira and D. H. S. Duarte, "Exploring the relationship between urban form, land surface temperature and vegetation indices in a subtropical megacity," (in English), *Urban Climate,* Article vol. 27, pp. 105-123, 2019.http://dx.doi.org/10.1016/j.uclim.2018.11.002

[33] C. B. Koc, P. Osmond, A. Peters, M. J. I. J. o. S. T. i. A. E. O. Irger, and R. Sensing, "Understanding land surface temperature differences of local climate zones based on airborne remote sensing data," vol. 11, no. 8, pp. 2724-2730, 2018.

[34] M. Morabito *et al.*, "Urban imperviousness effects on summer surface temperatures nearby residential buildings in different urban zones of Parma," (in English), *Remote Sensing,* Article vol. 10, no. 1, 2018, Art. no. 26.http://dx.doi.org/10.3390/rs10010026

[35] S. Mehrotra, R. Bardhan, and K. Ramamritham, "Urban Informal Housing and Surface Urban Heat Island Intensity," (in English), *Environment and Urbanization ASIA,* Article vol. 9, no. 2, pp. 158-177, 2018.http://dx.doi.org/10.1177/0975425318783548

[36] I. Agathangelidis, C. Cartalis, and M. Santamouris, "Urban morphological controls on surface thermal dynamics: A comparative assessment of major european cities with a focus on Athens, Greece," (in English), *Climate,* Article vol. 8, no. 11, pp. 1-33, 2020, Art. no. 131.http://dx.doi.org/10.3390/cli8110131

[37] C. Yin, M. Yuan, Y. Lu, Y. Huang, and Y. Liu, "Effects of urban form on the urban heat island effect based on spatial regression model," (in English), *Science of the Total Environment,* Article vol. 634, pp. 696-704, 2018.http://dx.doi.org/10.1016/j.scitotenv.2018.03.350

[38] D. Das Majumdar and A. Biswas, "Quantifying land surface temperature change from LISA clusters: An alternative approach to identifying urban land use transformation," (in English), *Landscape and Urban Planning,* Article vol. 153, pp. 51-65, 2016.http://dx.doi.org/10.1016/j.landurbplan.2016.05.001

[39] Y. A. Aina, E. M. Adam, and F. Ahmed, "Spatiotemporal variations in the impacts of urban land use types on urban heat island effects: The case of Riyadh, Saudi Arabia," 2017, vol. 42, pp. 9-14: International Society for Photogrammetry and Remote Sensing.

[40] I. M. Parvez, Y. A. Aina, and A. L. Balogun, "The influence of urban form on the spatiotemporal variations in land surface temperature in an arid coastal city," (in English), *Geocarto International,* Article vol. 36, no. 6, pp. 640-659, 2021.http://dx.doi.org/10.1080/10106049.2019.1622598

[41] RGPH, "Recenssement Générale de Population et de l'Habitat de 2014 - RGPH," *Haut-Commissariat au Plan du Maroc https://rgph2014.hcp.ma/downloads/Resultats-RGPH-2014_t18649.html (accessed 13 April 2021),* 2014.

[42] emines, "THE GREEN CITY OF BENGUERIR," *https://www.emines-ingenieur.org/en/life-at-emines/a-place-to-live/the-green-city-of-benguerir (accessed 27 March 2021),* 2012.

[43] J. K. Ord and A. Getis, "Local Spatial Autocorrelation Statistics: Distributional Issues and an Application," (in English), *Geographical Analysis,* Article vol. 27, no. 4, pp. 286-306, 1995.http://dx.doi.org/10.1111/j.1538-4632.1995.tb00912.x

[44] L. Anselin, "Local Indicators of Spatial Association-LISA," *Geographical Analysis,* https://doi.org/10.1111/j.1538-4632.1995.tb00338.x vol. 27, no. 2, pp. 93-115, 1995/04/01 2010.http://dx.doi.org/10.1111/j.1538-4632.1995.tb00338.x

[45] E. K. Mustafa *et al.*, "Study for Predicting Land Surface Temperature (LST) Using Landsat Data: A Comparison of Four Algorithms," (in English), *Advances in Civil Engineering,* Article vol. 2020, 2020, Art. no. 7363546.http://dx.doi.org/10.1155/2020/7363546

[46] A. Sekertekin and S. Bonafoni, "Land surface temperature retrieval from Landsat 5, 7, and 8 over rural areas: Assessment of different retrieval algorithms and emissivity models and toolbox implementation," (in English), *Remote Sensing,* Article vol. 12, no. 2, 2020, Art. no. 294.http://dx.doi.org/10.3390/rs12020294

[47] F. Liu, X. Jia, W. Li, A. Du, and D. Wang, "Analysis of Land Surface Temperature Evolution Based on Regional Road Scope," (in English), *Advances in Civil Engineering,* Article vol. 2020, 2020, Art. no. 4350787.http://dx.doi.org/10.1155/2020/4350787

[48] S. L. Ermida, P. Soares, V. Mantas, F. M. Göttsche, and I. F. Trigo, "Google earth engine open-source code for land surface temperature estimation from the landsat series," (in English), *Remote Sensing,* Article vol. 12, no. 9, 2020, Art. no. 1471.http://dx.doi.org/10.3390/RS12091471

[49] Z. Qin, A. Karnieli, and P. Berliner, "A mono-window algorithm for retrieving land surface temperature from Landsat TM data and its application to the Israel-Egypt border region," *International Journal of Remote Sensing,* vol. 22, no. 18, pp. 3719-3746, 2001/01/01 2010.http://dx.doi.org/10.1080/01431160010006971

[50] W. Choi, A. Moore, and P. Rasmussen, "Evaluation of temperature and precipitation data from NCEP-NCAR global and regional reanalyses for hydrological modeling in Manitoba," in *18th Canadian Hydrotechnical Conference, Winnipeg*, 2007.

[51] J. R. Lim, G. J. Snyder, C. K. Huang, J. A. Herman, M. A. Ryan, and J. P. Fleurial, "Thermoelectric microdevice fabrication process and evaluation at the Jet Propulsion Laboratory (JPL)," 2002, vol. 2002-January, pp. 535-539: Institute of Electrical and Electronics Engineers Inc.

[52] R. Wang, C. Ren, Y. Xu, K. K.-L. Lau, and Y. Shi, "Mapping the local climate zones of urban areas by GIS-based and WUDAPT methods: A case study of Hong Kong," (in English), *Urban Climate,* Article vol. 24, pp. 567-576, 2018.http://dx.doi.org/10.1016/j.uclim.2017.10.001

[53] B. Bechtel, L. See, G. Mills, and M. Foley, "Classification of Local Climate Zones Using SAR and Multispectral Data in an Arid Environment," (in English), *IEEE Journal of Selected Topics in Applied Earth Observations and Remote Sensing,* Article vol. 9, no. 7, pp. 3097-3105, 2016, Art. no. 7442773.http://dx.doi.org/10.1109/jstars.2016.2531420

[54] M. C. Hansen and T. R. Loveland, "A review of large area monitoring of land cover change using Landsat data," (in English), *Remote Sensing of Environment,* Review vol. 122, pp. 66-74, 2012.http://dx.doi.org/10.1016/j.rse.2011.08.024

[55] M. Pal, "Random forest classifier for remote sensing classification," (in English), *International Journal of Remote Sensing,* Article vol. 26, no. 1, pp. 217-222, 2007.http://dx.doi.org/10.1080/01431160412331269698

[56] d. T. N. Ministère de l'Amenagement, de l'Urbanisme, de l'Habitat et de la politique de la Ville. (2006, 25 Mai 2021). *Le programme national « villes sans bidonvilles » (VSB) (accessed 25 Mai 2021)*. Available: http://www.mhpv.gov.ma/?page_id=956

[57] OMM, "Le climat mondial 2011–2015," *Organisation météorologique mondiale https://library.wmo.int/doc_num.php?explnum_id=3104,* 2016.

[58] S. Haashemi, Q. Weng, A. Darvishi, and S. K. Alavipanah, "Seasonal variations of the surface urban heat Island in a semi-arid city," (in English), *Remote Sensing,* Article vol. 8, no. 4, 2016, Art. no. 352.http://dx.doi.org/10.3390/rs8040352

[59] M. Lazzarini, A. Molini, P. R. Marpu, T. B. M. J. Ouarda, and H. Ghedira, "Urban climate modifications in hot desert cities: The role of land cover, local climate, and seasonality," (in English), *Geophysical Research Letters,* Article vol. 42, no. 22, pp. 9980-9989, 2015.http://dx.doi.org/10.1002/2015GL066534

[60] A. Abulibdeh, "Analysis of urban heat island characteristics and mitigation strategies for eight arid and semi-arid gulf region cities," (in English), *Environmental Earth Sciences,* Article vol. 80, no. 7, 2021, Art. no. 259.http://dx.doi.org/10.1007/s12665-021-09540-7

[61] I. M. Parvez, Y. A. Aina, and A.-L. Balogun, "The influence of urban form on the spatiotemporal variations in land surface temperature in an arid coastal city," *Geocarto International,* vol. 36, no. 6, pp. 640-659, 2021/04/03 2021.http://dx.doi.org/10.1080/10106049.2019.1622598

[62] A. J. R. S. Getis and U. Economics, "Reflections on spatial autocorrelation," vol. 37, no. 4, pp. 491-496, 2007.

[63] A. Hilton and R. A. Armstrong, "Statnote 6: post-hoc ANOVA tests," *Microbiologist,* vol. 2006, pp. 34-36, 2006.

[64] P. Mohammad, A. Goswami, and S. Bonafoni, "The impact of the land cover dynamics on surface urban heat island variations in semi-arid cities: A case study in Ahmedabad City, India, using multi-sensor/source data," (in English), *Sensors (Switzerland),* Article vol. 19, no. 17, 2019, Art. no. 3701.http://dx.doi.org/10.3390/s19173701

[65] Z.-L. Li *et al.*, "Land surface emissivity retrieval from satellite data," *International Journal of Remote Sensing,* vol. 34, no. 9-10, pp. 3084-3127, 2013/05/01 2013.http://dx.doi.org/10.1080/01431161.2012.716540